Tunneling, $\alpha^2F(\omega)$, and transport in superconductors: Nb, V, VN, $Ba_{1-x}K_xBiO_3$, and $Nd_{1.85}Ce_{0.15}CuO_4$

N. Tralshawala,* J. F. Zasadzinski, L. Coffey, W. Gai,† and M. Romalis‡
Department of Physics, Illinois Institute of Technology, Chicago, Illinois 60616

Q. Huang, R. Vaglio,§ and K. E. Gray
Materials Science Division, Argonne National Laboratory, Argonne, Illinois 60439
(Received 30 June 1994)

The electron-phonon contribution to the normal-state resistivity, $\rho(T)$, has been calculated for the following conventional and oxide superconductors: Nb, V, VN, $Ba_{1-x}K_xBiO_3$, and $Nd_{1.85}Ce_{0.15}CuO_4$ (NCCO). The resistivity formula developed from the Boltzmann equation by Ziman and Allen is used, incorporating measured physical constants. The calculations are novel in that they incorporate the electron-phonon spectral function, $\alpha^2F(\omega)$, for each material as obtained from superconducting tunneling measurements, the same function that yields the superconducting transition temperature T_c. New tunneling and transport data are presented for VN. Fits to the experimental $\rho(T)$ are obtained over a wide temperature range with only two parameters: the plasma frequency ω_p, which is in good agreement with independent measurements and a saturation resistivity, ρ_s, which manifests itself at high temperatures. We find that the T-dependent normal state $\rho(T)$ is *completely* accounted for by phonon scattering in all materials except NCCO, where an additional electron-electron scattering term appears to be present. Apart from developing a consistent description of superconductivity and normal-state transport, several important issues are raised by the present work including indications of a conventional Fermi-liquid normal state in NCCO, insight into the importance of the shape of the Fermi surface in determining $\rho(T)$, and the role of high-energy optical phonons in oxide and nitride superconductors.

I. INTRODUCTION

Recent work[1-3] on the unusual normal-state properties of the cuprate oxide superconductors, in particular the linear normal-state resistivity $\rho(T)$ and the origin of their high-temperature superconducting state, underscores the need to develop a consistent description of both their normal and superconducting state properties. For example, models proposing antiferromagnetic spin fluctuations as a superconducting pairing mechanism will also yield normal-state quasiparticle scattering contributions to the resistivity. Theoretical work using magnetic-fluctuation-based pairing mechanisms has aimed at accounting quantitatively for both the magnitude and the linear temperature dependence of $\rho(T)$ in the cuprates, as well as the superconducting transition temperatures, within a strong-coupling formalism.[4,5] The role of electron-phonon scattering has not been factored into these analyses, however.

Superconducting tunneling measurements present an opportunity to address this last issue by providing, at least in some cases, the electron-phonon spectral weight $\alpha^2F(\omega)$ from a strong-coupling inversion procedure.[6] $\rho(T)$ can then be calculated using $\alpha^2F(\omega)$ in place of $\alpha^2_{tr}F(\omega)$, and a small number of experimentally measurable parameters such as the plasma frequency ω_P and the impurity contribution to the resistivity ρ_0. The measured superconducting transition temperature for the material can be predicted simultaneously using strong-coupling Eliashberg theory with the same $\alpha^2F(\omega)$ distribution. The result is a consistent understanding of the contribution of electron-phonon coupling to both the normal-state resistivity and superconducting state properties.

In the present work, normal-state resistivity curves for five superconducting materials, Nb, V, VN, $Ba_{1-x}K_xBiO_3$ (BKBO) and $Nd_{1.85}Ce_{0.15}CuO_4$ (NCCO) are fitted using a formula for $\rho(T)$, described in the next section of this paper, with the $\alpha^2F(\omega)$ obtained from inverting superconducting tunneling data on these materials. These $\alpha^2F(\omega)$ spectral functions can also be used to predict the correct superconducting transition temperatures for the same materials within the standard Eliashberg theory of superconductivity. Previous work on the cuprate oxide superconductor $Nd_{1.85}Ce_{0.15}CuO_4$ is presented for completeness.[7] The successful fitting of $\rho(T)$ for this selection of materials clearly demonstrates the validity of this approach and suggests that it may be useful in analyzing the phonon contribution to $\rho(T)$ in other cuprate oxide superconductors. In Sec. II, a discussion of the formula for $\rho(T)$ is presented, along with the $\alpha^2F(\omega)$ curves for the different materials analyzed here. In Sec. III, results are presented for $\rho(T)$, along with the values of parameters such as the plasma frequency ω_P and the high-temperature saturation resistivity ρ_s that are required to fit the data. Finally, a brief summary of the results is presented in Sec. IV.

II. THEORY

The contribution to the normal-state resistivity $\rho(T)$ due to electron-phonon scattering is calculated using the resistivity formula

$$\rho_{\rm ph}(T)=\frac{16\pi^2}{\omega_p^2}\frac{k_BT}{\hbar}\times\int_0^{\omega_{\rm ph}}\frac{d\omega}{\omega}\alpha_{\rm tr}^2F(\omega)\left[\frac{(\hbar\omega/2k_BT)}{\sinh(\hbar\omega/2k_BT)}\right]^2, \quad (1)$$

where $\omega_{\rm ph}$ is the cutoff frequency of the phonon spectrum, and the ω_p is the bare plasma frequency,

$$\omega_p^2=\frac{4\pi e^2}{3}2N(0)\langle v_F^2\rangle . \quad (2)$$

The electron-phonon transport function $\alpha_{\rm tr}^2F(\omega)$ is given by

$$\alpha_{\rm tr}^2F(\omega)=\left[\frac{\int dS_k}{|\mathbf{v}_k|}\right]^{-1}\int\frac{dS_k}{|\mathbf{v}_k|}\int\frac{dS_{k'}}{|\mathbf{v}_{k'}|}\frac{V}{(2\pi)^3\hbar}\sum_\nu|g_{k,k',\nu}|^2[1-\mathbf{v}_k\cdot\mathbf{v}_{k'}/|\mathbf{v}_k|^2]\delta(\hbar\omega-\hbar\omega_{\nu,k-k'}) , \quad (3)$$

where $g_{k,k',\nu}$ is the electron-phonon coupling constant, $\mathbf{v}_k$ is the group velocity of state $\mathbf{k}$ and the integration $\int dS_k$ denotes an integration over the Fermi surface for the material in question.

Equation (1) for $\rho(T)$ was developed by Ziman from the Boltzmann equation using a variational technique and by Allen who rewrote the expression for $\rho(T)$ in terms of the $\alpha_{\rm tr}^2F(\omega)$ function.[8–10] For simplicity, we refer to Eq. (1) as the Ziman formula in the remainder of this paper.

At temperature $k_BT\geq\hbar\omega_{\rm ph}$, the resistivity can be written as

$$\rho_{\rm ph}(T)=\frac{8\pi^2k_B}{\hbar}\frac{\lambda_{\rm tr}}{\omega_p^2}T , \quad (4)$$

where $\lambda_{\rm tr}$ is defined as

$$\lambda_{\rm tr}=2\int_0^{\omega_{\rm ph}}(d\omega/\omega)\alpha_{\rm tr}^2F(\omega) .$$

Inversion of superconducting tunneling data yields the phonon spectral weight function[6]

$$\alpha^2F(\omega)=\left[\int\frac{dS_k}{|\mathbf{v}_k|}\right]^{-1}\times\int\frac{dS_k}{|\mathbf{v}_k|}\int\frac{dS_k'}{|\mathbf{v}_{k'}|}\frac{V}{(2\pi)^3\hbar}\times\sum_\nu|g_{k,k',\nu}|^2\delta(\hbar\omega-\hbar\omega_{\nu,k-k'}) , \quad (5)$$

The electron-phonon coupling constant λ generalization of the BCS critical temperature formula is given by

$$\lambda=2\int_0^{\omega_{\rm ph}}\frac{\alpha^2F(\omega)}{\omega}d\omega . \quad (6)$$

The expressions for $\alpha_{\rm tr}^2F(\omega)$ and $\alpha^2F(\omega)$ are quite similar, except for the factor $[1-\mathbf{v}_k\cdot\mathbf{v}_{k'}/|\mathbf{v}_k|^2]$ which preferentially weights backscattering processes. Use of $\alpha^2F(\omega)$ instead of $\alpha_{\rm tr}^2F(\omega)$ in the Ziman formula is generally believed to result in no significant quantitative error.[11,12] However, there can exist a significant difference between λ and $\lambda_{\rm tr}$ for the case of a strongly nested Fermi surface,[13] with $\lambda_{\rm tr}$ being significantly smaller than λ due to the contribution from backscattering of electrons between opposite sides of a nested Fermi surface. This issue clearly affects the use of the slope of the high temperature $\rho(T)$ to extract a value for λ for use in the strong-coupling transition temperature expression and also may render it difficult to fit the low-temperature behavior of $\rho(T)$ accurately. We discovered that we were able to *completely* account for the measured $\rho(T)$ in Nb, V, VN, and BKBO using the tunneling $\alpha^2F(\omega)$ and values of ω_p which were in good agreement with other experiments and calculations. This indicates that despite the complex Fermi surfaces in these materials, there does not exist a substantial difference between λ and $\lambda_{\rm tr}$.

In addition to the electron-phonon interaction, electrons also scatter off impurities, defects, and disordered regions and this gives rise to a temperature-independent contribution to the resistivity, ρ_0, which can be determined from each $\rho(T)$ by extrapolation to zero temperature. A typical metallic resistivity curve has distinct shapes in four different temperature regions. (i) At very low temperatures, it exhibits a power-law behavior, i.e., $\rho\propto T^n$, where n typically has values between 2 and 5.[3] (ii) Next, there is a turnover region where the resistivity changes from power law to a linear shape. (iii) In the intermediate temperature range, the resistivity varies linearly with temperature. (iv) At very high temperatures, the resistivity starts to saturate toward a value denoted by ρ_s which is determined in the fitting of $\rho(T)$.

The total resistivity $\rho(T)$ is modeled with the expression[14]

$$[\rho(T)]^{-1}=[\rho_0+\rho_{\rm ph}(T)]^{-1}+[\rho_s]^{-1} . \quad (7)$$

The value of ρ_0 is determined by extrapolating the resistivity data to $T=0$. Hence, we essentially have only two fitting parameters, ω_p and ρ_s, and the shape of the resistivity data in the linear and the saturation region yields a unique pair of values of these two parameters to fit the data. The fitted plasma frequency can then be compared to the band-structure calculations and/or the optical/IR reflectance data, where available. We can relate the saturation resistivity, ρ_s with the smallest physical mean free

path, l_s as[1,14]

$$\rho_l l_s = 4.95 \times 10^{-4} v_F \omega_p^{-2} , \tag{8}$$

where ρ_s is expressed in $\mu\Omega$ cm, l_s in Å, v_F in cm/s and ω_p in eV. We then insert values of v_F obtained from other independent measurements and calculations into this equation, along with the fitted values of ω_p and ρ_s to obtain l_s and compare it to the lattice nearest-neighbor distance,[14] which corresponds to the physical limit on the electronic mean free path due to the electron-phonon interaction. Our overall procedure is similar to that of Allen and co-workers[11,12] except that we use the experimentally measured values of $\alpha^2F(\omega)$ rather than model expressions.

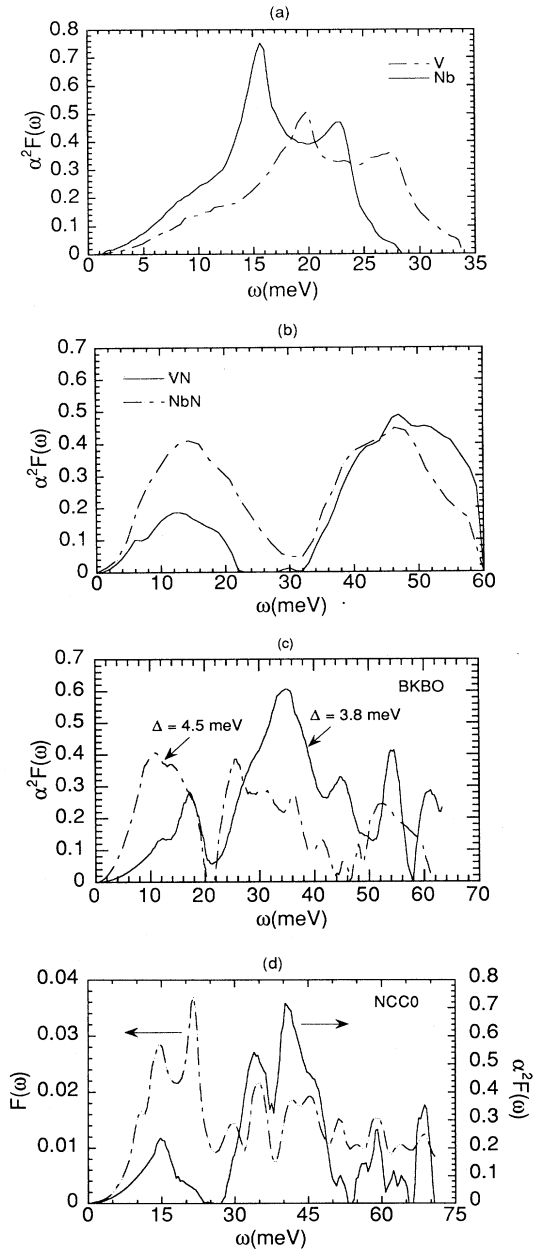

FIG. 1. Compilation of tunneling $\alpha^2F(\omega)$ for (a) Nb (solid line) and V (dot-dashed line), (b) VN (solid line) and NbN (Ref. 17) (dot-dashed line), (c) two BKBO junctions: BKB-2 (solid line) and BKB-5 (dot-dashed line), and (d) NCCO junction-2 (Ref. 18) (solid line), and the phonon density of states $F(\omega)$ generated from the dispersion curves obtained from the inelastic neutron scattering on single-crystal NCCO (Ref. 20) (dot-dashed line).

The $\alpha^2F(\omega)$ spectral functions obtained from inverting the tunneling measurements and used in fitting $\rho(T)$ are shown in Fig. 1. $\alpha^2F(\omega)$ results are shown in Fig. 1(a) for the conventional superconductors Nb (Ref. 15) and V,[16] in Fig. 1(b) for the binary compounds, NbN (Ref. 17) and VN, where optical phonons are important for the superconductivity, in Fig. 1(c) for two BKBO junctions,[18] which agree with the phonon spectral density $G(\omega)$ obtained from neutron-scattering data,[19] and in Fig. 1(d) NCCO $\alpha^2F(\omega)$, along with $F(\omega)$.[18,20] A final point to be made about our analysis is that there is a minor source of error at low temperatures (≤ 120 K) due to the fact that the tunneling $\alpha^2F(\omega)$ is forced to go as ω^2 for very low frequencies.[6,21] This leads to a T^3 dependence of $\rho(T)$ whereas the measured data will be proportional to T^n with $n=2-5$ depending on such factors as sample purity.[3]

III. ANALYSIS OF NORMAL-STATE RESISTIVITY

Nb and V

Nb and V are conventional superconductors, with only low-frequency, acoustic phonons involved in establishing superconductivity. Measured resistivity for both Nb and V (Ref. 22) up to 2000 K is shown in Fig. 2 along with

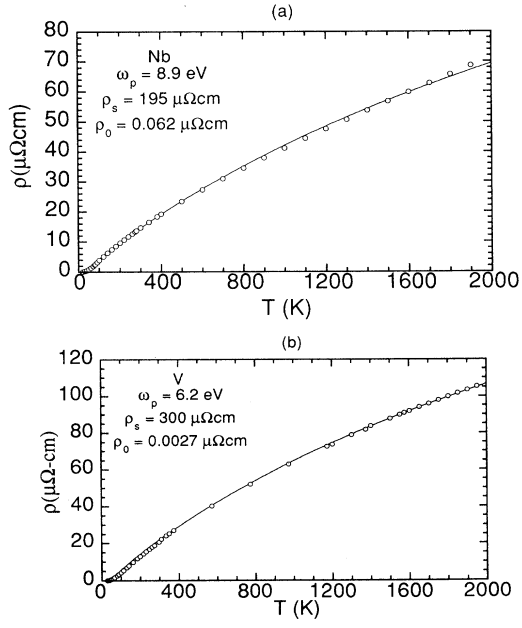

FIG. 2. Nb and V resistivity: Fitting parameters shown in the top left corner of the figures. Solid line is the fit to the data represented by open symbols.

the fit calculated using the procedure outlined in the previous section. The overall agreement between the fit and the data is excellent with a maximum discrepancy of 20% found at 80 K for Nb and at 120 K for V which may be traced to the ω^2 dependence of $\alpha^2F(\omega)$ at low frequencies as discussed above. We use 8.9 eV for the plasma frequency of Nb, obtained from band-structure calculations,[12] in the resistivity calculation and hence require only *one* free parameter, ρ_s when fitting the experimentally measured $\rho(T)$. Using the band-structure Fermi velocity,[12] 6.1×10^7cm/s and the ρ_s of 195 $\mu\Omega$ cm, we obtain a saturation mean free path of 1.95 Å from Eq. (7), which compares reasonably to the nearest-neighbor distance of 2.85 Å in Nb.[23]

For V, we use v_F of 5.2×10^7 cm/s, calculated from the specific-heat and magnetization measurements.[24] Using the coefficient of electronic specific heat for V, $\gamma=1.179\times10^4$ erg cm^{-3} K^{-2},[24] we obtain the electronic density of states at the Fermi energy, $N(0)$.[25] Equation (2) yields a plasma frequency of 6.6 eV. In fitting $\rho(T)$ for V, Fig. 2(b), a plasma frequency of 6.2 eV is required, which compares favorably with the previous calculation. Using the values of $\omega_p=6.2$ eV and $\rho_s=300$ $\mu\Omega$ cm and the calculated Fermi velocity, $v_F\, l_s$ is calculated to be 2.3 Å, compared to the nearest-neighbor distance of 2.62 Å in V.[23]

The Nb and V data are shown in Fig. 3 but in this case only up to 300 K. It is worth noting that there is little evidence of saturation effects in the data when this limited temperature range is examined. To emphasize this point, a fit is included (solid line) which uses the same ω_p as in Fig. 2 but which ignores the saturation term, i.e., $\rho_s=\infty$. The weak saturation effect is due to the relatively large ratio $\rho_s/\rho_{\rm ph}$ (300 K) which is 13 and 15 in Nb and V, respectively, and therefore the effect of the parallel saturation resistance is small in this temperature range. An improved fit to the data up to 300 K could be obtained by ignoring the saturation term and choosing a slightly higher plasma frequency in each case. The conclusion would nevertheless be the same, that is, phonon scattering alone accounts for all the temperature-dependent normal-state electronic transport.

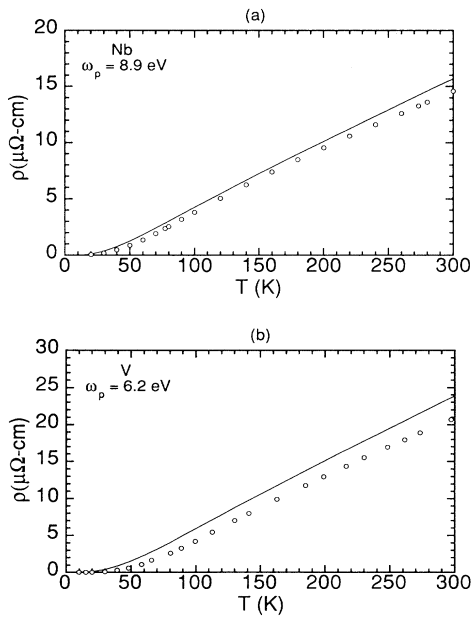

FIG. 3. Resistivity of Nb and V (open symbols) up to 300 K compared to $\rho_{\rm ph}$, excluding saturation.

There are two points to be made here. First, the absence of obvious saturation effects over a limited temperature range does not rule out phonon scattering by any means. Second, when the data appear linear, a fit to the Ziman expression for $\rho(T)$ [Eq. (1)] with reasonable parameters can be obtained by ignoring ρ_s. We will address this issue again when considering BKBO and NCCO data. It is also worth noting that although the Fermi surfaces of Nb and V are quite complex,[24,26] the analysis using $\alpha^2F(\omega)$ instead of $\alpha^2_{\rm tr}F(\omega)$ in Eq. (1) produces an accurate fit to the experimentally measured resistivity along with reasonable values for ω_p, ρ_0, and ρ_s. This observation lends support to proceeding in the same manner when fitting $\rho(T)$ for BKBO and NCCO even though the Fermi surfaces of both BKBO (Ref. 27) and NCCO (Ref. 28) are closer to being nested than being spherical.

VN

We have made well-ordered, stoichiometric films of VN by reactive sputtering and have studied the effects of disordering due to the deviation from stoichiometry ($VN_x, x\leq1$) and radiation damage.[29,30] Tunneling data have been obtained with all-thin-film junctions on well-ordered samples using MgO as the tunnel barrier. High-bias data showed characteristic phonon structure that was inverted using a modified McMillan-Rowell procedure,[6] and the $\alpha^2F(\omega)$ is shown in Fig. 1(b).

VN is very similar in structure and properties to another $B1$ compound, NbN, and high-energy optical phonons appear to play an important role in establishing superconductivity in both materials.[17] As Fig. 1 shows, the agreement in shape and magnitude of the high-frequency part of $\alpha^2F(\omega)$ (30–60 meV) in NbN and VN is striking and appears to resolve a controversy surrounding the observation of such modes in NbN.[17,31]

Two as-made VN films with widely varying degrees of disorder (as indicated by the resistivity ratio) were chosen for resistivity measurements. Film VN-2 was measured up to 600 K in a tube furnace under flowing nitrogen gas. The results are shown in Fig. 4. The solid lines are the fit to the data using the Ziman formula, Eq. (1), and our measured $\alpha^2F(\omega)$. The ω_p and ρ_s values obtained from the fits are almost identical even though the ρ_0 values differ by an order of magnitude. This result is consistent with the fact that T_c changes little with disorder[29,30] and verifies our assumption that $\alpha^2F(\omega)$ is essentially the same for both films. Similarly, the phonon contribution to the resistivity remains constant for VN samples with widely varying amounts of disorder.

We use a value for v_F of 2×10^7 cm/s obtained from critical field measurements.[29] Using this value and the $N(0)$ obtained from magnetic-susceptibility data[26] in Eq.

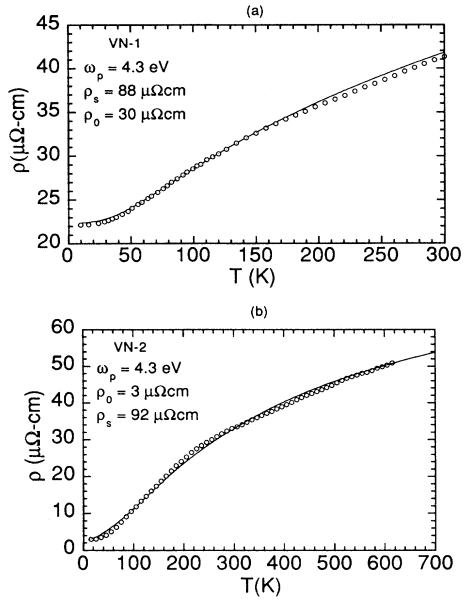

FIG. 4. VN resistivity: Fitting parameters shown in the top left corner of the figures. Solid line is the fit to the data represented by open symbols.

(2), we obtain $\omega_p = 4.8$ eV which is close to the fitted value of 4.3 eV. Using the fitted value of ρ_s and ω_p along with the v_F value obtained from critical field measurements, we get, for l_s a value of 6 Å, compared to the lattice constant[29] of 4.13 Å. Note that if the larger $\omega_p = 4.8$ eV is used, then $l_s = 4.8$ Å is obtained, in better agreement with the lattice constant. Another uncertainty results from the estimate of v_F from critical field measurements[29] and this could account for the larger l_s as well. The effect of saturation in the resistivity data is very obvious (the ratio ρ_s/ρ_{300}^{ph} is about 3).

This analysis shows that the tunneling and transport procedure outlined in Sec. I works well in explaining the resistivity in VN and means that we have extended our procedure to include a binary compound where the optical part of the tunneling $\alpha^2F(\omega)$ function is important. Furthermore, our analysis of $\rho(T)$ for Nb, V, and VN indicates that it is very difficult to infer and account for the presence of saturation in the resistivity data up to only 300 K unless the ratio ρ_s/ρ_{300}^{ph} is small. This point is important to bear in mind when we look at the BKBO and NCCO data, which are available only up to 300 K.

BKBO

BKBO is a cubic, isotropic superconductor and has optical-phonon modes involved in superconductivity similar to VN [see Fig. 1(c)]. The density of states in the superconducting gap region, obtained through tunneling measurements, displays ideal behavior and can be fitted with a BCS model.[18] The tunneling $\alpha^2F(\omega)$ compares well with the phonon density of states obtained from the inelastic neutron-scattering data,[19] and the T_c obtained from tunneling $\alpha^2F(\omega)$ (Ref. 18) matches well with the measured value. The resistivity data sets of BKBO reported in the literature have ranged from semiconducting to metallic.[32] Good, grain-boundary free epitaxial thin films and single crystals of BKBO, which are doped away from the charge-density-wave (CDW) instability, exhibit metallic resistivity, whereas grainy films and the ceramic samples exhibit semiconducting behavior.

Two different $\alpha^2F(\omega)$ functions[18] obtained from two BKBO junctions are illustrated in Fig. 1(c). Junction BKB-2 has a lower gap value, $\Delta_0 = 3.8$ meV compared to that of the other junction, BKB-5, where $\Delta_0 = 4.5$ meV. Here we use the sample notation of Ref. 18. The $\alpha^2F(\omega)$ curve obtained from junction BKB-5, has more spectral weight at the low-frequency end of the spectrum compared to that of the BKB-2 curve. We expect that the calculated resistivity resulting from BKB-5 will have a narrower power-law region than that calculated from BKB-2. This is due to the fact that the Fermi factors inside the integral of Eq. (1) will more quickly exhaust most of the spectral weight of the $\alpha^2F(\omega)$ and the limiting, linear condition expressed in Eq. (4) is obtained for lower temperatures. The $\alpha^2F(\omega)$ for the BKB-2 junction, which results in a lower superconducting gap, implies that the tunneling measurements were obtained from the region on the BKBO surface that was further away from the CDW instability,[33] resulting in a T_c that was reduced from the optimum value. Hence the $\alpha^2F(\omega)$ from junction BKB-2 should be more appropriate for fitting the metallic resistivity.

From a compilation of various reported resistivity data[32] on thin-film and bulk BKBO samples, the best metallic data set has $\rho_{300} - \rho_0$ of about 175 μΩ cm. This corresponds to a $Ba_{1-x}K_xBiO_3$ with $x = 0.466$ and $T_c = 16.9$ K. We use this data set to carry out our analysis. The fitting is depicted in Fig. 5. The fit using the BKB-2 $\alpha^2F(\omega)$ is in excellent agreement with the data with a maximum discrepancy of $\leq 10\%$ at 120 K. Attempts to fit the data with the BKB-5 $\alpha^2F(\omega)$ were less successful and in order to fit the magnitude of the linear portion of

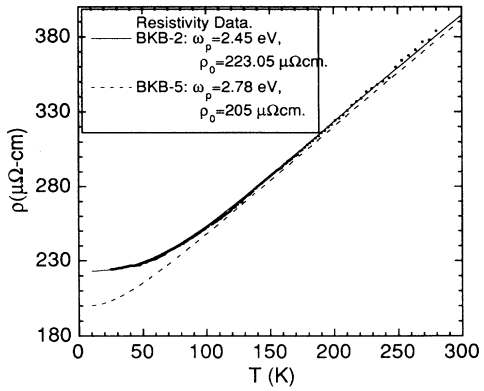

FIG. 5. Fitting the BKBO resistivity. The data are fitted to the calculated resistivities from junctions BKB-2 and BKB-5. The plasma frequency deduced from the fits is shown in the inset. Fit from BKB-5 is shifted down by 5 μΩ cm for clarity.

the data, we had to relax the constraint on ρ_0, allowing it to be an adjustable parameter. Note also that the linearity sets in at a lower T using the BKB-5 $\alpha^2F(\omega)$ due to the larger spectral weight at lower frequencies. This is in disagreement with the data. The improved fit with the BKB-2 $\alpha^2F(\omega)$ especially for $T \leq 100$ K points to the importance of the shape of $\alpha^2F(\omega)$ as well as the total integrated weight expressed in λ. The dominant feature of the BKB-2 $\alpha^2F(\omega)$ is the strong spectral weight in the region of the higher-energy optical phonons (30–60 meV).

The fitted plasma frequency value agrees well with the value deduced from optical conductivity measurements[34] on BKBO. The ω_p values vary with x. Extrapolating the ω_p value for $x=0.466$ from Fig. 1 of Ref. 34, we obtained a renormalized $\omega_p \simeq 1.8$ eV. Using the λ value of 0.99 obtained for junction BKB-2, we obtained a bare plasma frequency of 2.54 eV which is very close to the fitted value of 2.45 eV. Note that the fit of the BKBO data ignored any saturation effects. Visual observation of the data shows no evidence of saturation and a more quantitative justification for ignoring ρ_s for BKBO can be given as follows. Band-structure calculations[27] give $v_F = 4.7 \times 10^7$ cm/s. Using this value of v_F, $\omega_p = 2.45$ eV and the Bi-O bond length in BKBO for l_s, (2.15 Å), we obtain an estimate of $\rho_s = 1800\ \mu\Omega$ cm, about 10 times the value of ρ_{ph} at 300 K. This suggests that the BKBO resistivity up to 300 K is only weakly affected by saturation effects, similar to what is found in Nb and V. Therefore, a proper experimental determination of ρ_s for BKBO would require $\rho(T)$ data up to much higher temperatures.

We would also like to point out that Hellman and Hartford[32] have analyzed the same resistivity data using an extended Einstein mode model where all the spectral weight is uniformly distributed at low frequencies and requiring three free parameters for the fit. On the other hand, we use experimentally obtained $\alpha^2F(\omega)$ to calculate resistivity using a more rigorous Ziman resistivity formula based on the Bloch-Boltzmann theory. Our analysis requires only one fitting parameter, ω_p, whose value, as we show, agrees well with independent optical measurements.[34] In essence, we do not have any free parameters in our analysis. To our knowledge, this is the first such connection of normal-state and superconducting-state experimental data for any oxide superconductor. It demonstrates first that BKBO has a Fermi-liquid normal state and that phonons are principally responsible for both superconductivity and normal-state transport. Finally, it should be noted that Samuely *et al.*[35] have recently obtained $\alpha^2F(\omega)$ from junctions on BKBO samples with $T_c \simeq 18$ K. Their results are quite similar to the BKB-2 junction of Fig. 1(c).

NCCO

Experimental measurements of $\rho(T)$ for $Nd_{1.85}Ce_{0.15}CuO_4$ for three different samples are presented in Fig. 6.[36–38] Calculated phonon contributions to $\rho(T)$, using the experimentally measured $\alpha^2F(\omega)$ shown in Fig. 1(d), are represented by the solid lines in Fig. 6. This analysis has been published previously[7] and is being included here to emphasize the ability of the present fitting procedure to reveal potentially interesting nonphonon-related contributions to $\rho(T)$. Furthermore, new optical measurements of ω_p exist for NCCO with which to compare our analysis. The NCCO $\rho(T)$ data was fitted with an expression of the form

$$\rho(T) = \rho_0 + \rho_{ph}(T) + \rho_{ee}(T) \ . \tag{9}$$

The experimental $\rho(T)$ shows no evidence of resistivity saturation and so the ρ_s parameter does not enter this particular analysis. When the best obtainable electron-phonon contribution to $\rho(T)$ is subtracted from the experimentally measured $\rho(T)$, a T^2 Fermi-liquid-like contribution remains, denoted by $\rho_{ee}(T)$. It was observed[7] that the increase in the magnitude of this contribution correlated reasonably well with the values for the fitted plasma frequencies. The T^2 contribution is shown in Fig. 7 for the three samples shown in Fig. 6 and is detectable

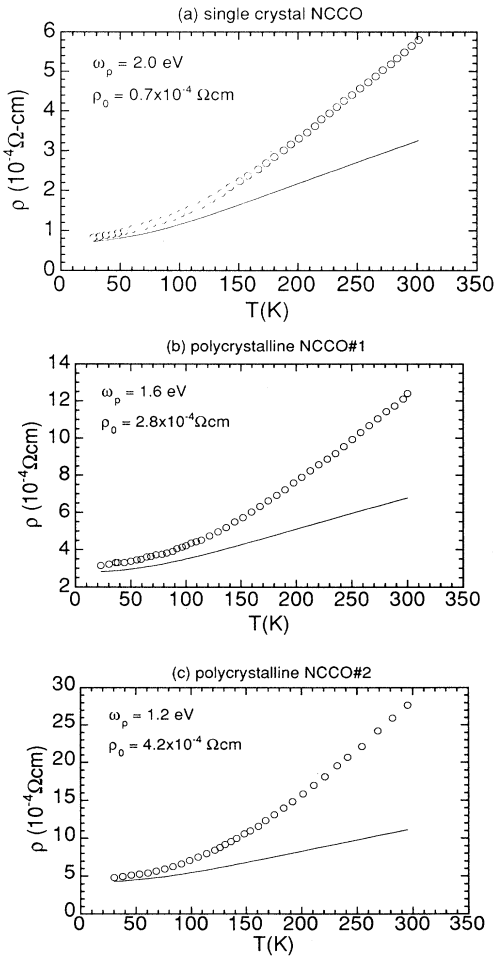

FIG. 6. The experimental data for (a) the single crystal, and (b) and (c) the two thin-film NCCO samples are plotted as open symbols. The solid lines are the phonon contribution to the resistivity from Eq. (1). Also shown on each plot are the temperature independent values for ρ_0 due to disorder and of the plasma frequency ω_p used in calculating the phonon contribution.

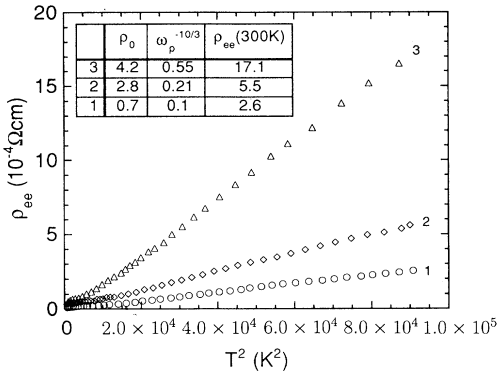

FIG. 7. The NCCO experimental resistivity plotted as a function of T^2 after $\rho_0+\rho_{ph}(T)$ is subtracted off. The inset shows the values of $(\omega_p)^{-10/3}$ for the three samples and the value of the T^2 contribution at $T=300$ K.

due to the low carrier concentration in these NCCO samples. The values obtained for ω_p in fitting the NCCO data fall in the range 1–2 eV. This is consistent with the infrared data of Ref. 39 where a renormalized plasma frequency of about 1 eV is obtained. Using $\lambda \simeq 1$, this leads to a bare plasma frequency of 1.42 eV. This observation has an important bearing on speculation about the possibility of a non-Fermi-liquid normal state in the cuprate oxide superconductors. The ability to subtract off, convincingly, the electron-phonon contribution to the measured $\rho(T)$ clearly plays a significant role in this whole analysis.

The presence of the large $\rho_{ee}(T)$ term in NCCO makes it difficult to say anything quantitative about the relationship between λ and λ_{tr} and the role of Fermi-surface nesting. For example, if $\alpha^2F(\omega)_{tr}$ was indeed smaller than $\alpha^2F(\omega)$, say by 40% over the whole spectral range, then the same fit to the data would be obtained with a smaller ω_p (about 20% smaller) which would still be in the range of acceptable values based on the optical data. This is in contrast to Nb, V, VN, and BKBO where the analysis clearly indicates that $\alpha^2F(\omega)_{tr}$ and $\alpha^2F(\omega)$ are very similar despite the complexities of the Fermi surfaces.

IV. CONCLUSIONS

We have successfully shown that one can use the $\alpha^2F(\omega)$ spectral function obtained from superconducting tunneling to fit $\rho(T)$ of conventional superconductors like Nb, V, the intermetallic $B1$ compound, VN, as well as the oxide superconductor BKBO. High-temperature saturation of $\rho(T)$ is accounted for. The parameter ρ_s/ρ_{300}^{ph} determines whether the resistivity saturation can be observed at room temperature or not. The higher the value of ρ_s/ρ_{300}^{ph}, the less likely it is that the resistivity data only up to room temperature will be sufficient to determine whether resistivity saturation occurs. We have shown that the resistivity measurements of BKBO can be explained completely using the tunneling $\alpha^2F(\omega)$, indicating that BKBO behaves like a conventional Fermi liquid and that superconductivity in BKBO is due to electron-phonon coupling.

The presence of high-energy optical-phonon modes, arising from oxygen vibrations, in both the cuprate oxides and BKBO, as well as the proximity of BKBO to a CDW phase[33] and the cuprate oxides to a spin-density-wave phase,[40] suggest intriguing similarities between these two systems. One displays conventional s-wave superconductivity (BKBO) whereas the high-temperature superconducting state of the cuprate oxides is believed to be unconventional. Furthermore, our analysis suggests that conventional electron-phonon scattering makes an important contribution to the normal-state resistivity in NCCO, that a conventional Fermi-liquid state may be a valid description of the normal state of this material, and that one cannot work backwards from the measured $\rho(T)$ for NCCO to a prediction of the superconductor transition temperature for this material.

In summary, we have illustrated how information from superconducting tunneling experiments, specifically the electron-phonon spectral function, can be used to develop a consistent, quantitative description of resistivity in several important low-temperature and a cuprate oxide superconducting material.

ACKNOWLEDGMENTS

We wish to thank Eric Hellman for sending the BKBO resistivity data prior to its publication. This work was supported in part by the Illinois Department of Energy and Natural Resources Grant No. SC-5 (N.T.). The work was also partially supported by the U. S. Department of Energy, Division of Basic Energy Sciences-Materials Sciences (K.E.G.) under Contract No. W-31-109-ENG-38 and the National Science Foundation, Office of Science and Technology Centers (J.F.Z. and Q.H.) under Contract No. DMR 91-2000.

*Present address: Texas Center for Superconductivity, University of Houston, Houston, TX 77204.
†Present address: High Energy Physics Division, Argonne National Laboratory, Argonne, IL 60439.
‡Present address: Department of Physics, Princeton University, Princeton, NJ 08544.
§Present address: Dipartimento di Scienze Fisiche, Universita di Napoli, Napoli, Italy.

[1]M. Gurvitch and A. T. Fiory, Phys. Rev. Lett. **59**, 1337 (1987).
[2]C. M. Varma, P. B. Littlewood, S. Schmitt-Rink, E. Abrahams, and A. E. Ruckenstein, Phys. Rev. Lett. **63**, 1996 (1989); P. W. Anderson and Z. Zou, Phys. Rev. Lett. **60**, 132 (1988).
[3]M. Gurvitch, Physica C **135B**, (1985).
[4]P. Monthoux and D. Pines, Phys. Rev. B **47**, 6069 (1993).
[5]R. J. Radtke, S. Ullah, K. Levin, and M. Norman, Phys. Rev. B **46**, 11 975 (1992).
[6]E. L. Wolf, *Principles of Electron Tunneling Spectroscopy* (Oxford, New York, 1985).

[7]N. Tralshawala, J. F. Zasadzinski, L. Coffey, and Q. Huang, Phys. Rev. B **44**, 12 102 (1991).
[8]G. Grimvall, *The Electron-Phonon Interaction in Metals* (North-Holland, Amsterdam, 1981).
[9]P. B. Allen, Phys. Rev. B **3**, 305 (1971).
[10]J. M. Ziman, *Electrons and Phonons: The Theory of Transport Phenomena in Solids* (Oxford University Press, New York, 1960).
[11]P. B. Allen and Werner W. Schulz, Phys. Rev. B **47**, 14 434 (1993).
[12]P. B. Allen, T. P. Beaulac, F. S. Khan, W. H. Butler, F. J. Pinski, and J. C. Swihart, Phys. Rev. B **34**, 4331 (1986).
[13]V. H. Crespi and M. L. Cohen, Solid State Commun. **81**, 187 (1992).
[14]M. Gurvitch, Phys. Rev. B **24**, 7404 (1981).
[15]G. B. Arnold, J. F. Zasadzinski, J. W. Osmun, and E. L. Wolf, J. Low Temp. Phys. **40**, 225 (1980).
[16]J. F. Zasadzinski, Ph. D. thesis, Iowa State University, 1980.
[17]K. E. Kihlstrom, R. W. Simon, and S. A. Wolf, Physica **135B**, 198 (1985).
[18]Q. Huang, J. F. Zasadzinski, N. Tralshawala, K. E. Gray, D. G. Hinks, J. L. Peng, and R. L. Greene, Nature (London) **347**, 369 (1990).
[19]C. K. Loong, P. Vashishta, R. K. Kalia, M. H. Degani, D. L. Price, J. D. Jorgensen, D. G. Hinks, B. Dabrowski, A. W. Mitchell, D. R. Richards, and Y. Zheng, Phys. Rev. Lett. **62**, 2628 (1989).
[20]W. Reichardt, F. Gompf, L. Pintschovius, N. Pyka, B. Renker, P. Bourges, G. Collin, A. S. Ivanov, N. L. Mitrofanov, and A. Yu. Rumiantsev, in *Electron-Phonon Interaction in Oxide Superconductors,* edited by R. Baquero (World Scientific, Singapore, 1991).
[21]W. L. McMillan and J. M. Rowell, Phys. Rev. Lett. **14**, 108 (1965); and W. N. Hubin, Tech. Rep. 182 ARPA SD-31, (1970), University of Illinois, Urbana.
[22]J. Bass, in *Metals: Electronic Transport Phenomena,* edited by K. H. Hellwege, *Landolt-Börnstein Tables,* New Series, Group 3, **15**, Part a, Sec. 1.2.2 (Springer, Berlin, 1982).
[23]N. W. Ashcroft and N. D. Mermin, *Solid State Physics* (Saunders, New York, 1976).
[24]R. Radebaugh and P. H. Keesom, Phys. Rev. **149**, 217 (1966).
[25]H. Rietschel, Phys. Rev. B **24**, 155 (1981).
[26]F. I. Ajami and R. K. MacCrone, J. Phys. Chem. Solids **36**, 7 (1975).
[27]L. F. Mattheiss and D. R. Hamann, Phys. Rev. Lett. **60**, 2681 (1988).
[28]D. M. King *et al.*, Phys. Rev. Lett. **70**, 3159 (1993).
[29]K. E. Gray, R. T. Kampwirth, D. W. Capone II, R. Vaglio, and J. Zasadzinski, Phys. Rev. B **38**, 2333 (1988).
[30]J. F. Zasadzinski, R. Vaglio, G. Rubino, K. E. Gray, and M. Russo, Phys. Rev. B **32**, 2929 (1985).
[31]J. Geerk, U. Schneider, W. Bangert, H. Rietschel, F. Gompf, M. Gurvitch, J. Remeika, and J. M. Rowell, Physica **135B**, 187 (1985).
[32]E. S. Hellman and E. H. Hartford, Jr., Phys. Rev. B **47**, 11 346 (1993).
[33]S. Pei, N. J. Zaluzec, J. D. Jorgensen, B. Dabrowski, D. G. Hinks, A. W. Mitchell, and D. R. Richards, Phys. Rev. B **39**, 811 (1989); D. G. Hinks, B. Dabrowski, D. R. Richards, J. D. Jorgensen, S. Pei, and J. F. Zasadzinski, Physica C **162-164**, 1405 (1989).
[34]M. A. Karlow, S. L. Cooper, A. L. Kotz, M. V. Klein, P. D. Han, and D. A. Payne, Phys. Rev. B **48**, 6499 (1993).
[35]P. Samuely, N. L. Bobrov, A. G. M. Jansen, P. Wyder, S. N. Barilo, and S. V. Shiryaev, Phys. Rev. B **48**, 13 904 (1993).
[36]C. C. Tseui, Physica A **168**, 238 (1990).
[37]Y. Hidaka and M. Suzuki, Nature (London) **338**, 635 (1989).
[38]A. Gupta, G. Koren, C. C. Tsuei, A. Segmüller, and T. R. McGuire, Appl. Phys. Lett. **55**, 1795 (1989).
[39]W. E. Hughes, Y. Lu, T. Timusk, and J. S. Preston, Phys. Rev. B **47**, 985 (1993).
[40]J. D. Jorgensen, H.-B. Schüttler, D. G. Hinks, D. W. Capone, II, K. Zhang, and M. B. Brodsky, Phys. Rev. Lett. **58**, 1024 (1987).